Molecular Pharmacology Fast Forward. Published on January 16, 2018 as DOI: 10.1124/mol.117.110767
This article has not been copyedited and formatted. The final version may differ from this version.

Assay Conditions Influence Affinities of Rat Organic Cation Transporter 1: Analysis of Mutagenesis in the Modeled Outward-facing Cleft by Measuring Effects of Substrates and Inhibitors on Initial Uptake.

Valentin Gorboulev, Saba Rehman, Christoph M. Albert, Ursula Roth, Marleen J. Meyer, Mladen V. Tzvetkov, Thomas D. Mueller, and Hermann Koepsell

Institute of Anatomy and Cell Biology, University of Würzburg, 97070 Würzburg, Germany (V.G.,S.R. C.M.A., U.R. H.K.); Institute of Clinical Pharmacology, University Medical Center, Georg-August University Göttingen, Germany (M.J.M., M.V.T.); Department of Molecular Plant Physiology and Biophysics, Julius-von-Sachs-Institute, University of Würzburg, 97082 Würzburg, Germany (T.D.M., H.K.)

Running title: Two Amino Acids in OCT1 Bind to Extracellular Inhibitors

Address correspondence to: Hermann Koepsell, Department of Molecular Plant Physiology and Biophysics, Julius-von-Sachs-Institute, Julius-von-Sachs-Platz 2, 97082 Würzburg, Germany, phone +49 931 3182700; fax +49 931 31-82087; E-mail: Hermann@Koepsell.de

Number of text pages: 18

Number of tables: 4

Number of figures: 8

Number of references: 42

Number of words in the abstract: 243

Number of words in the introduction: 746

Number of words in the discussion: 1432

ABBREVIATIONS: OCT, organic cation transporter; rOCT, rat organic cation transporter; hOCT, human organic cation transporter; MFS, major facilitator superfamily; TEA^+, tetraethylammonium$^+$; MPP^+, 1-methyl-4-phenylpyridinium$^+$; $TBuA^+$, tetrabutylammonium$^+$; $TPeA^+$, tetrapentylammonium$^+$; HEK, human embryonic kidney; IC_{50}, half-maximal concentration for inhibition; 3D model, three-dimensional model

Molecular Pharmacology Fast Forward. Published on January 16, 2018 as DOI: 10.1124/mol.117.110767
This article has not been copyedited and formatted. The final version may differ from this version.

ABSTRACT

Effects of mutations in the modeled outward-open cleft of rat organic cation transporter 1 (rOCT1) on affinities of substrates and inhibitors were investigated. Human embryonic kidney (HEK) 293 cells were stably transfected with rOCT1 or rOCT1 mutants, and uptake of the substrates 1-methyl-4-phenylpyridinium$^+$ (MPP^+) and tetraethylammonium$^+$ (TEA^+) or inhibition of MPP^+ uptake by the non-transported inhibitors tetrabutylammonium$^+$ ($TBuA^+$), tetrapentylammonium$^+$ ($TPeA^+$) and corticosterone was measured. Uptake measurements were performed on confluent cell layers using 2 min-incubation or in dissociated cells using incubation times of 1, 5, or 10 s. With both methods different apparent Michaelis-Menten K_m values, different half-maximal inhibitor concentrations (IC_{50}), and varying effects of mutations were determined. In addition, varying IC_{50} values for inhibition of MPP^+ uptake and varying effects of mutations were obtained when different MPP^+ concentrations far below the apparent K_m value were used for uptake measurements. Eleven mutations were investigated by measuring initial uptake in dissociated cells and employing 0.1 µM MPP^+ for uptake during inhibition experiments. Altered affinities for substrates and/or inhibitors were observed when Phe160, Trp218, Arg440, Leu447 and Asp475 were mutated. The mutations resulted in changes of apparent K_m values for TEA^+ and/or MPP^+. Mutation of Trp218 and Asp475 led to altered IC_{50} values for $TBuA^+$, $TPeA^+$ and corticosterone, whereas mutation of Phe160 and Leu447 changed the IC_{50} values for two inhibitors. Thereby amino acids in the outward-facing conformation of rOCT1 could be identified that interact with structurally different inhibitors and probably also with different substrates.

Molecular Pharmacology Fast Forward. Published on January 16, 2018 as DOI: 10.1124/mol.117.110767
This article has not been copyedited and formatted. The final version may differ from this version.

Introduction

Organic cation transporters OCT1, OCT2 and OCT3 (*SLC22A1-3*) of the major facilitator superfamily MFS play pivotal roles in the absorption, excretion, and tissue distribution of many cationic drugs including psychopharmaca and cytostatics (Koepsell et al., 2007; Nies et al., 2010; Koepsell, 2013; Lin et al., 2015; Chen et al., 2017; Ahlin et al., 2008). The polyspecificity of OCTs explains their predominant role for drug bioavailability and the high probability for drug-drug interactions at the transporter level. The identification of drugs that are transported by OCTs or inhibit OCTs has become an important issue in pharmacology. For example, *in vitro* testing of human OCT1 (hOCT1) for drug-drug interactions has been recommended in 2015 by the European Medicines Agency. Although methods to identify new substrates and inhibitors of OCTs have been established, so far no satisfying strategies for *in silico* and/or *in vitro* distinction between substrates and inhibitors and for elucidation of biomedical relevant effects of transporter polymorphisms have been found (Chen et al., 2017; Koepsell, 2015). The reasons are that the transport mechanism(s) of OCTs is(are) not fully understood, no crystal structures are available, and our molecular understanding of cation binding and translocation based on mutagenesis is very limited.

Previously we investigated transport mechanisms of OCT1 and OCT2 expressed in oocytes of *Xenopus laevis*. We provided evidence that these transporters are polyspecific facilitated diffusion systems that can operate as electrogenic uniporters or as electroneutral cation exchangers (Busch et al., 1996b; Budiman et al., 2000; Arndt et al., 1998; Volk et al., 2003; Koepsell, 2011). Studying structure-function relationships in rat OCT1 (rOCT1) we determined effects of several single point mutations on affinities of substrates and inhibitors (Gorboulev et al., 1999; Gorboulev et al., 2005; Popp et al., 2005; Volk et al., 2009). We interpreted these data with the help of homology models obtained using the crystal structure of bacterial *Lac permease* transporter, which belongs to the MFS superfamily (Abramson et al., 2003; Pao et al., 1998), as template. To determine the effects of mutations on the affinities of tetraethylammonium$^+$ (TEA^+) and 1-methyl-4-phenylpyridinium$^+$ (MPP^+) uptake and on uptake inhibition by the non-transported inhibitors corticosterone and tetrabutylammonium$^+$ ($TBuA^+$), rOCT1 mutants expressed in oocytes were characterized by measuring uptake of radioactive substrates or substrate-induced inward-currents. For inhibition

Molecular Pharmacology Fast Forward. Published on January 16, 2018 as DOI: 10.1124/mol.117.110767
This article has not been copyedited and formatted. The final version may differ from this version.

studies, we measured uptake of radioactive substrates using substrate concentrations below the apparent K_m value and a 30 min-incubation time or substrate-induced inward-current using substrate concentrations above the apparent K_m and a 45 sec-incubation time. For molecular interpretations we made simplifying assumptions, e.g. that the effects of mutations in the modeled outward-open cleft on affinities of the inhibitors indicate inhibitor interactions with the mutated amino acids. We became concerned whether interpretations which were based on uptake measured after 30 min-incubation, hold true because these measurements are not supposed to represent a defined transport mode.

During recent years increasing evidence has been obtained that indicate complex structure-function relationships in OCTs which allow direct and indirect interactions between structurally different substrates and/or inhibitors. Thus, organic cation transporters contain low-affinity and high-affinity binding sites, and cation binding to these sites may lead to direct cation replacement and/or allosteric interactions (Minuesa et al., 2009; Gorbunov et al., 2008; Koepsell, 2011; Koepsell, 2015). Different affinities of inhibitors of hOCT1 and human OCT2 (hOCT2) were determined when different substrates were used for the uptake measurement (Ahlin et al.,2011; Thevenod et al., 2013; Belzer et al., 2013). In addition, different affinities for inhibition of hOCT2 were obtained when 2-min uptake measurements were performed in confluent cells versus 1 s-uptake measurements in dissociated cells (Thevenod et al., 2013).

In the present study we show that mutations of individual amino acids in rOCT1 may have quite different effects on apparent K_m values of MPP^+ and TEA^+ uptake, and on half-maximal concentration values for inhibition (IC_{50}) of MPP^+ uptake when different experimental conditions are used in the uptake measurements. To identify amino acids that interact with the non-transported inhibitors $TBuA^+$, corticosterone and tetrapentylammonium$^+$ ($TPeA^+$) we analysed effects of various mutations of amino acids located in the outward-open cleft of our three-dimensional (3D) homology model on IC_{50} values of uptake under *trans*-zero conditions. The measurements were performed in stably transfected, dissociated human embryonic kidney (HEK) 293 cells using a 1, 5 or 10 s-incubation time and a fixed low MPP^+ concentration for uptake in inhibition studies. The obtained data suggest that five amino acids in the outward-open cleft interact with TEA^+ and/or MPP^+ and indicate that four of these interact with $TBuA^+$, $TPeA^+$ and/or corticosterone.

Molecular Pharmacology Fast Forward. Published on January 16, 2018 as DOI: 10.1124/mol.117.110767
This article has not been copyedited and formatted. The final version may differ from this version.

Materials and Methods

Materials. [^{3}H]MPP$^+$ (3.1 TBq/mmol) and [^{14}C]TEA$^+$ (1.9 GBq/mmol) were purchased from American Radiolabeled Chemicals (St. Louis, MO). All other chemicals were obtained as described earlier (Arndt et al., 2001; Popp et al., 2005; Tzvetkov et al., 2012).

Cloning. For expression in oocytes and transfection of HEK293 cells, wildtype rOCT1 (Gründemann et al., 1994) and rOCT1 mutants (Popp et al., 2005; Volk et al., 2009) were cloned into various vectors. The single point mutations were generated by polymerase chain reaction applying the overlap extension method (Ho et al., 1989) and all mutations were verified by DNA sequencing. For expression in oocytes, wildtype rOCT1 and rOCT1 mutants were cloned into vector pRSSP (Busch et al., 1996b). For transfection of HEK293 cells, rOCT1 and mutants were cloned into EcoRV/NotI sites of vector pcDNA3.1 (Egenberger et al., 2012) or into EcoRV/HindIII sites of the vector pcDNA5.1 (Tzvetkov et al., 2012).

Expression of rOCT1 and rOCT1 Mutants in Oocytes of *Xenopus laevis*. pRSSP plasmids were purified and linearized with MluI. m7G(5´)ppp(5´)G-capped cRNAs were prepared and the cRNA concentrations were estimated from ethidium bromide-stained agarose gels (Gründemann and Koepsell, 1994). Stage V-VI oocytes of *Xenopus laevis* were obtained by partial ovariectomy, follical cells were removed by treatment with collagenase A, and oocytes were stored in Ori buffer (5 mM MOPS, 100 mM NaCl, 3 mM KCl, 2 mM $CaCl_2$, 1 mM $MgCl_2$ adjusted to pH 7.4 using NaOH) supplemented with 50 mg/liter gentamycin. The oocytes were injected with 50 nl H_2O containing 10 ng cRNA encoding the transporters. For transporter expression, the oocytes were incubated 3 days at 16^{o}C in Ori buffer containing 50 mg/ml gentamicin.

Measurement of MPP$^+$ Uptake in Oocytes. Transporter expressing oocytes or control oocytes without cRNA injection were incubated for 30 min at room temperature with Ori buffer containing varying concentrations of TEA$^+$ traced with [^{14}C]TEA$^+$, varying concentrations of MPP$^+$ traced with [^{3}H]MPP$^+$ or 0.1 µM MPP$^+$ traced with [^{3}H]MPP$^+$ plus varying concentrations of TEA$^+$ or TBuA$^+$. Oocytes were washed with ice-cold Ori-buffer, solubilized with 5% SDS in water and the radioactivity was analysed by liquid scintillation counting. Correction for nonspecific uptake was performed by subtracting uptake rates measured in non-injected control oocytes from the same batch of oocytes.

Molecular Pharmacology Fast Forward. Published on January 16, 2018 as DOI: 10.1124/mol.117.110767
This article has not been copyedited and formatted. The final version may differ from this version.

Generation and Cultivation of Stably Transfected Human Embryonic Kidney (HEK293) cells. HEK293 cells were transfected with vector pcDNA5.1 or pcDNA3.1 containing rOCT1 wildtype and rOCT1 mutants and selected for stably transfected cell lines as described (Busch et al., 1996a). Cell lines exhibiting the highest saturable MPP^+ uptake were used for further studies. The cells were cultivated at 37°C in Dulbecco´s modified Eagle´s medium containing 3.7 g/liter $NaHCO_3$, 1.0 g/liter D-glucose, 2 mM L-glutamine, 10% heat-inactivated fetal calf serum, 100,000 units/liter penicillin, 100 mg/liter streptomycin, and 0.8 g/liter geneticin (G418). Cultivation was performed in a humidified atmosphere containing 5% CO_2.

Two Min-Uptake Measurements of MPP^+ in Monolayers of HEK293 Cells at 37°C. HEK293 cells which were stably transfected with vector pcDNA5.1 containing wildtype rOCT1, the rOCT1 mutants Y222F or D475E or human organic cation transporter 1 (hOCT1), were cultivated in six-well plates until reaching confluence. After washing 2 times with 137 mM NaC1, 2.7 mM KCl, 8 mM Na_2HPO4, 1.6 mM KH_2PO_4, pH 7.4 (PBS) supplemented with 0.5 mM $MgCl_2$ and 1 mM $CaCl_2$ (Mg-Ca-PBS) (37°C), the monolayers were incubated for 2 min at 37°C with Mg-Ca-PBS containing varying concentrations of MPP^+ traced with [^{3}H]MPP^+, TEA^+ traced with [^{14}C]TEA^+, or 0.1 µM MPP^+ traced with [^{3}H]MPP^+ plus varying concentrations of TEA^+, MPP^+ or $TBuA^+$. Uptake was stopped by washing with ice-cold PBS, cells were solubilized with 0.2 ml 4M guanidine thiocyanate and analysed for radioactivity.

Measurements of Initial Uptake Rates in Dissociated HEK293 Cells at 37°C. HEK293 cells stably transfected with vector pcDNA3.1 containing rOCT1 or rOCT1 mutants were cultivated until confluence. The cells were washed twice with PBS and suspended in the same buffer by shaking at room temperature. The cells were collected by centrifugation (10 min, 1000×g) and suspended (10^8 cells/ml) at 37°C in Mg-Ca-PBS. Initial uptake rates in HEK293 cells expressing wildtype rOCT1 and most mutants were measured after incubation for 1 s with radioactively traced MPP^+ or for 10 s with radioactively traced TEA^+. In HEK293 cells expressing mutant rOCT1(D475E), which has a largely reduced transport activity compared to wildtype rOCT1 (Gorboulev et al. 1999), MPP^+ uptake was measured after 5 s-incubation with substrates. To measure inhibition of MPP^+ uptake by TEA^+, $TBuA^+$, $TPeA^+$ or corticosterone, the inhibitors were added together with MPP^+. Using these

incubation times, the measurements are supposed to represent *trans*-zero substrate uptake, and passive diffusion of $TPeA^+$ and corticosterone was supposed to be neglectable. To perform the short-time uptake measurements, 90 µl of HEK293 cell suspension was placed at the bottom of 2-ml tubes and mixed by agitation in a water bath at 37°C. The uptake measurements were performed tube by tube employing a switched-on vortexing-device and a metronome providing a 1s-tact. 10 µl of Mg-Ca-PBS buffer containing 1 mg/ml albumin and the appropriate concentration of inhibitor and/or radioactive and nonradioactive substrate was placed on the inner wall of the tube about 0.5 cm above the surface of the cell suspension. Albumin was added to increase the adhesion of the radioactive solution to the reaction vessel. Uptake measurement was started by mixing the solutions. For uptake measurements the tube was added to the vortexer and stopped by addition of 1 ml of ice-cold stop solution after 1, 5 or 10 seconds indicated by the metronome. The stop solution consisted of PBS containing 100 µM quinine. After two centifugation/washing steps with ice-cold stop solution, cell pellets were solubilized with 0.2 ml 4 M guanidine thiocyanate. Two ml scintillation liquid was added and radioactivity was determined by liquid scintillation counting.

Statistics and Fitting Procedures. For uptake measurements of $[^3H]MPP^+$ or $[^{14}C]TEA^+$ into oocytes at least three different experiments employing different batches of oocytes were used. In each experiment 8-10 oocytes were analysed per experimental condition. For determination of uptake rates of MPP^+ or TEA^+ into HEK293 cells at least three different experiments were performed. In each experiment four individual measurements were performed per experimental condition. The software package GraphPad Prism Version 4.1 (GraphPad Software, San Diego) was used to compute statistical parameters. Apparent K_m values were determined by fitting the Michaelis-Menten equation (Table 1, Fig. 1A) or the Hill equation (Tables 2 and 3, Figs. 2-4) to substrate-activation measurements. The data are presented as replacement of radioactive by non-labeled substrate to avoid large scatter at high substrate concentrations. The employed equations are indicated in Supplementary Fig. 1. In wildtype rOCT1 and most mutants the obtained Hill coefficient was not statistically significantly different from one, and similar apparent K_m values were determined using the Michaelis-Menten or Hill equation. Attempts to fit the two-site-competition model indicated in Supplementary Fig. 1 to the substrate replacement curves did not resolve two sites and did not improve the goodness of the fit. Half-

Molecular Pharmacology Fast Forward. Published on January 16, 2018 as DOI: 10.1124/mol.117.110767
This article has not been copyedited and formatted. The final version may differ from this version.

maximal concentration values for inhibition of [^{3}H]MPP$^+$ transport (IC_{50}) by substrates and non-transported inhibitors were determined by fitting the Hill equation to the data after subtracting uptake that could not be inhibited by the highest employed concentration of the respective compound (see equation in Supplementary Fig. 1). Fitting the two-site-competition model shown in Supplementary Fig. 1 to the inhibition data did not resolve two inhibitory sites. The presented apparent K_m values and IC_{50} values represent means ± S.D. which were obtained by fitting data from individual experiments. The curves indicated in Figs. 2-7 were obtained by fitting the Hill equation to data of the compiled experiments. In the presented graphs individual data points are presented as mean values ± S.D. from 3 or 4 individual experiments. When more than two groups were compared the statistical significance of differences was determined by ANOVA using post hoc Tukey comparison. Student´s t-test was used for evaluation of statistical significance of difference between two groups. $P < 0.05$ was considered statistically significant.

Results

Impact of Experimental Conditions on Affinities of rOCT1 for Substrates and Inhibitors and on Effects of Mutations on Affinities. Largely different apparent K_m values and IC_{50} values for substrates and inhibitors of OCT1 were determined in various laboratories using different expression systems and/or different experimental conditions for transport measurements (Koepsell et al., 2007; Nies et al., 2010). In different expression systems, such as *Xenopus laevis* oocytes and epithelial cells, transporters may exist in diverging regulatory states. Using different incubation times for tracer uptake measurements may determine whether *trans-zero* cation import or net uptake of cation import minus cation export is analysed. Tracer uptake in epithelial cells and cation-induced inward-currents in voltage-clamped oocytes may record transport activity at different membrane potentials. When testing inhibitor affinities using different substrates, it turned out that the substrate properties may influence the IC_{50} values (Ahlin et al., 2011; Thevenod et al., 2013; Belzer et al., 2013). Previously we characterized functional activities of wildtype rOCT1 and rOCT1 mutants expressed in oocytes of *Xenopus laevis* by measuring tracer flux uptake after 30 min-incubation at room temperature (Gorboulev et al., 1999; Popp et al., 2005) and by measuring cation-induced inward-currents in

Molecular Pharmacology Fast Forward. Published on January 16, 2018 as DOI: 10.1124/mol.117.110767
This article has not been copyedited and formatted. The final version may differ from this version.

voltage-clamped oocytes (Volk et al., 2009). We also measured the effects of a few mutations on initial rates of tracer flux at 37°C in stably transfected HEK293 cells (Egenberger et al., 2012). In other laboratories functional analysis of human OCT1 (hOCT1) was performed in stably transfected HEK293 cells by measuring tracer flux uptake in confluent cells using incubation times of several minutes (Matthaei et al., 2016; Nies et al., 2009; Chen et al., 2010; Tzvetkov et al., 2012).

In the present study we compared apparent K_m values and IC_{50} values of wildtype rOCT1 as well as variants rOCT1(Y222F) and rOCT1(D475E) in HEK293 cells and oocytes using different conditions for the uptake measurements. We measured apparent K_m values for uptake of TEA^+ and MPP^+, and IC_{50} values for inhibition of uptake of 0.1 µM MPP^+ by TEA^+ or $TBuA^+$. Apparent K_m values and IC_{50} values of wildtype rOCT1 and the two rOCT1 mutants are presented in Table 1, and the effects of the mutations on apparent K_m values and IC_{50} values are shown in Fig. 1. Uptake was determined at 37°C in stably transfected HEK293 cells or at room temperature in oocytes. We analysed initial uptake rates in dissociated HEK293 cells or uptake after 2-min incubation in confluent cell layers of HEK293 cells. For measurements of initial uptake rates incubation times of 1 s (MPP^+ uptake by wildtype rOCT1 and rOCT1(Y222F)), 5 s (MPP^+ uptake by rOCT1(D475E)), and 10 s (TEA^+ uptake) were used. In oocytes, the transporter was expressed by cRNA injection and uptake of radioactive MPP^+ was measured after 30-min incubation.

For wildtype rOCT1 similar apparent K_m values for TEA^+ or MPP^+ were determined in dissociated HEK293 cells and in oocytes, whereas the apparent K_m values measured in confluent HEK293 cells were 5-6fold (TEA^+ uptake) or 16-20fold (MPP^+ uptake) higher (Table 1). The IC_{50} value for inhibition of rOCT1-mediated uptake of 0.1 µM MPP^+ by TEA^+ measured in confluent HEK293 cells was 15 times higher than in dissociated HEK293 cells and 5 times higher than in oocytes (Table 1). For inhibition of rOCT1-mediated uptake of 0.1 µM MPP^+ by $TBuA^+$, an about 8 times lower IC_{50} value was determined in dissociated HEK293 cells compared to confluent HEK293 cells or compared to oocytes (Table 1).

Noteworthy we observed that experimental conditions used for uptake measurements also influenced the determined functional effects of the mutations. In mutant Y222F the apparent K_m for TEA^+ uptake measured in dissociated HEK293 cells was similar to wildtype rOCT1 whereas it was

Molecular Pharmacology Fast Forward. Published on June 26, 2018 as DOI: 10.1124/mol.117.110767
This article has not been copyedited and formatted. The final version may differ from this version.

strongly decreased when uptake was measured in oocytes (Fig. 1A left panel). Replacement of Asp475 by glutamate (mutant D475E) lead to a similar strong decrease of the apparent K_m value for TEA^+ uptake determined in dissociated HEK293 cells and oocytes (Fig. 1A left panel). The Y222F mutation did not alter the apparent K_m value for MPP^+ measured in dissociated or confluent HEK293 cells but induced an increase in apparent K_m in oocytes (Fig. 1A right panel). In the D475E mutant compared with wildtype, the apparent K_m for MPP^+ uptake was not changed in dissociated HEK293 cells while it was decreased by different degrees in confluent HEK293 cells and oocytes (Fig. 1A right panel). In mutant Y222F, the IC_{50} value for inhibition of MPP^+ uptake by TEA^+ was decreased compared to wildtype rOCT1 in dissociated HEK293 cells and oocytes while it was not changed in confluent HEK293 cells (Fig. 1B left panel). At variance, upon exchange of Asp475 with glutamate, the IC_{50} value for inhibition of MPP^+ uptake by TEA^+ was not changed when analysed in dissociated HEK293 cells while it was strongly decreased when determined in confluent HEK293 cells and oocytes (Fig. 1B right panel). Due to the Y222F mutation, the IC_{50} value for inhibition of MPP^+ uptake by $TBuA^+$ was decreased to different degrees in dissociated and confluent HEK293 cells but not changed in oocytes (Fig. 1C left panel). Upon replacement of Asp475 by glutamate, the IC_{50} for inhibition of MPP^+ uptake by $TBuA^+$ was halved in dissociated HEK293 cells and decreased by more than 90% in confluent HEK293 cells and oocytes (Fig. 1C right panel).

Influence of the Substrate Concentration on the IC_{50} Values of Inhibitors. Since rOCT1 contains high- and low-affinity cation binding sites (Gorbunov et al., 2008), we asked whether the inhibitors may inhibit cation transport with different affinities when different substrate concentrations far below their respective apparent K_m value are used for uptake measurements. In HEK293 cells stably transfected with rOCT1, rOCT1(Y222F) or rOCT1(D475E) we therefore measured inhibition of 1 s-uptake (rOCT1, rOCT1(Y222F)) or 5 s-uptake (rOCT1(D475E)) of 0.25 nM MPP^+, 12.5 nM MPP^+ or 0.1 µM MPP^+ by various concentrations of $TBuA^+$ and calculated the IC_{50} values by fitting the Hill equation to the data (Fig. 2, Table 2). Employing the three different MPP^+ concentrations, three different IC_{50} values were obtained for rOCT1 and rOCT1(D475E) while the IC_{50} values determined for rOCT1(Y222F) were similar at all three MPP^+ concentrations. Interestingly the IC_{50} values determined for rOCT1 and rOCT1(D475E) using 12.5 nM MPP^+ were lower compared to the values

Molecular Pharmacology Fast Forward. Published on January 16, 2018 as DOI: 10.1124/mol.117.110767
This article has not been copyedited and formatted. The final version may differ from this version.

determined with 0.1 µM MPP^+ or 0.25 nM MPP^+. Under most conditions a Hill coefficient around one was determined, however, Hill coefficients lower than one were obtained for inhibition of uptake of 12.5 nM MPP^+ by wildtype rOCT1 and for inhibition of uptake of 0.25 nM MPP^+ by rOCT1(D475E) (Fig. 2). Assuming that the effects of the different MPP^+ concentrations (all of which are far below the apparent K_m value of MPP^+) are due to different interactions with high-affinity MPP^+ binding sites, the data suggests that interactions with two high-affinity MPP^+ binding sites are involved. The negative cooperativity observed under some conditions suggests that $TBuA^+$ binds to two binding sites that interact under the respective conditions. Using different MPP^+ concentrations for the uptake measurements we also observed different effects of mutations on the efficacy of $TBuA^+$ inhibition. The mutation Y222F decreased the IC_{50} value for $TBuA^+$ inhibition of uptake of 0.1 µM MPP^+ compared to wildtype rOCT1, but did not alter the IC_{50} value for $TBuA^+$ inhibition of uptake of 12.5 nM MPP^+ or 0.25 nM MPP^+ (Table 2). On the other hand, the mutation D475E decreased the IC_{50} for $TBuA^+$ inhibition of uptake of 0.1 µM and 12.5 nM MPP^+ but increased the IC_{50} for $TBuA^+$ inhibition of uptake of 0.25 nM MPP^+.

Effects of Mutations in rOCT1 on Apparent K_m Values for MPP^+ and TEA^+ Determined from Initial Uptake Rates in Transfected HEK293 Cells. Measuring inhibition of TEA^+-induced currents by corticosterone in oocytes expressing rOCT1 mutants, we previously identified five amino acids (Phe160, Trp218, Arg440, Leu447, Asp475) which are located in the outward-open cleft of our three-dimensional (3D) structural model and influence the efficacy of corticosterone for inhibition of TEA^+ uptake (Volk et al., 2009). Performing 30 min-uptake measurements of TEA^+ and MPP^+ in oocytes expressing wildtype rOCT1 and mutants W218F and D475E, we observed that replacement of Asp475 by glutamate changed the apparent K_m for TEA^+ uptake whereas replacement of Trp218 by phenylalanine did not alter the apparent K_m values for TEA^+ and MPP^+ (Gorboulev et al., 1999; Popp et al., 2005). To study the functional significance of Phe160, Trp218, Arg440, Leu447 and Asp475 in the outward-facing cleft of our 3D structural model under optimal experimental conditions, we analysed mutants F160A, F160Y, W218L, W218F, W218Y, R440K, L447F, L447Y and D475E on *trans-zero* uniport transport activity by measuring initial uptake rates of MPP^+ and TEA^+ in dissociated, stably transfected HEK293 cells. Replacements of Phe160 by tyrosine or alanine, of

Molecular Pharmacology Fast Forward. Published on January 16, 2018 as DOI: 10.1124/mol.117.110767
This article has not been copyedited and formatted. The final version may differ from this version.

Trp218 by phenylalanine, tyrosine or leucine, and of Leu447 by phenylalanine or tyrosine were performed to determine effects of slightly and distinctly different structural changes. We also investigated effects of mutations Y222F and T226A because uptake measurements in oocytes revealed effects on apparent K_m values for TEA^+ and/or MPP^+ by these mutations although in our 3D structural models these amino acids were only found accessible in the inward-open cleft (Popp et al. 2005; Volk et al., 2009).

In HEK293 cells the apparent K_m value for MPP^+ determined by fitting the Hill equation to the data was increased when Phe160 was exchanged by alanine or tyrosine while the apparent K_m value for TEA^+ was not changed (Table 3, Figs. 3A and 4A). Whereas Hill coefficients around one were determined for MPP^+ uptake by wildtype rOCT1 and mutant F160A and for TEA^+ uptake by wildtype rOCT1 and mutants F160A and F160Y, a negative cooperativity was obtained for MPP^+ uptake by mutant F160Y (Figs. 3A and 4A). In HEK293 cells stably transfected with mutant W218Y the apparent K_m value for MPP^+ uptake was strongly decreased compared to wildtype rOCT1 and a negative cooperativity was induced whereas the apparent K_m and Hill coefficient for TEA^+ uptake remained unaltered (Table 3, Figs. 3B and 4B). When Trp218 was replaced by phenylalanine, the apparent K_m value for MPP^+ uptake and the Hill coefficient remained unchanged, however, the apparent K_m value for TEA^+ uptake was increased. In mutant W218L no statistically significant TEA^+ uptake could be detected whereas the apparent K_m for MPP^+ uptake was increased. The apparent K_m values for MPP^+ and TEA^+ uptake and the respective Hill coefficients were not altered when Tyr222 was replaced by phenylalanine (Table 3, Figs. 3C and 4C). In mutant T226A compared to wildtype, the apparent K_m for MPP^+ uptake was increased and a negative cooperativity was induced whereas the apparent K_m and Hill coefficient for TEA^+ uptake remained unchanged (Table 3, Figs. 3C and 4C). In mutants R440K, L447F, L447Y and D475E compared to wildtype, the apparent K_m value for MPP^+ uptake remained unchanged, however, a negative cooperativity was induced in D475E (Table 3, Figs. 3C, D). The apparent K_m value for TEA^+ uptake compared to wildtype was decreased in mutants R440K and D475E, increased in mutant L447F and unchanged in mutant L447Y. The respective Hill coefficient was increased in mutant R440K and not altered in mutants L447F, L447Y and D475E (Table 3, Fig. 4C, D). Considering that Phe160, Trp218, Arg440, Leu447 and Asp475 have been

Molecular Pharmacology Fast Forward. Published on January 16, 2018 as DOI: 10.1124/mol.117.110767
This article has not been copyedited and formatted. The final version may differ from this version.

located in our 3D models to the outward- and inward-open binding cleft whereas Thr226 has been only assigned to the inward-open cleft (Volk et al., 2009; Popp et al., 2005), and assuming that extracellular substrate binding rather than intracellular substrate dissociation determines the apparent K_m measured under *trans*-zero conditions (see discussion), the data may be interpreted as follows: The effects of the mutations of Trp218 on apparent K_m values for MPP^+ and TEA^+ uptake suggest that Trp218 interacts directly with both substrates in the outward-open cleft. Direct interaction of MPP^+ with Phe160 in the outward-open cleft is also suggested by the effects of mutations on the apparent K_m values for MPP^+ uptake, whereas direct interactions of TEA^+ with Arg440, Leu447 and Asp475 are suggested by altered K_m values observed for TEA^+ uptake. The Hill coefficients different from one observed for MPP^+ uptake in mutants F160Y, W218Y and D475E suggest the existence of two transport-relevant binding sites for MPP^+ in which cooperative interactions are induced by the respective mutations. The effect of the mutation of Thr226 on the K_m for MPP^+ uptake may be due to an allosteric effect on substrate binding to the outward-open cleft.

Different Effects of Mutations in rOCT1 on IC_{50} Values for Inhibition of MPP^+ Uptake by TEA^+ versus Apparent K_m Values of TEA^+ Uptake. Measurements with rOCT1, rOCT1(Y222F) and rOCT1(D475E) presented in Table 1 indicate that under identical experimental conditions partially different values were determined for the apparent K_m of TEA^+ uptake versus the respective IC_{50} value for inhibition of 0.1 µM MPP^+ uptake by TEA^+. In some cases, different effects of mutagenesis on the apparent K_m value versus the respective IC_{50} value were observed. These data indicate complex interactions between MPP^+ and TEA^+ that are influenced by single point mutations. To evaluate the impact of all investigated mutations on these interactions between MPP^+ and TEA^+, we also measured the IC_{50} values for inhibition of uptake of 0.1 µM MPP^+ by TEA^+ after mutation of Phe160, Trp218, Thr226, Arg440 or Leu447. The data obtained for wildtype rOCT1 and all investigated mutants are shown in Supplemental Fig. 4. In Supplemental Table 1 a comparison between the IC_{50} values for TEA^+ inhibition of MPP^+ uptake and the apparent K_m values for TEA^+ uptake is presented. In wildtype rOCT1 the IC_{50} value is 37% smaller than the apparent K_m value. For mutants F160A, W218F, W218Y, R440K and L447Y similar IC_{50} and apparent K_m values were determined whereas 2.7-3.8fold diverging IC_{50} and apparent K_m values were obtained for mutants

F160Y, Y222F, T226A, L447F and D475E. In consequence these mutations induced different effects on the IC_{50} and apparent K_m values. Whereas for inhibition of MPP^+ uptake by TEA^+ in wildtype rOCT1 and most mutants a Hill coefficient around one was determined, positive cooperativity was observed for mutant F160Y and negative cooperativity for mutants W218L, T226A and L447F (Supplemental Fig. 4). The observations suggest effects of mutations of Phe160, Tyr222, Thr226, Leu447 and Asp475 on simultaneous binding of TEA^+ and MPP^+ which allows mutual direct and/or allosteric interactions between the two substrates.

Effects of Mutations in rOCT1 on IC_{50} Values for Inhibition of MPP^+ Uptake by Non-transported Inhibitors. Next, we determined whether the above mentioned mutations in rOCT1 influence the inhibition of 1 or 5 s-uptake of 0.1 µM MPP^+ by $TBuA^+$, $TPeA^+$ and corticosterone (Figs. 5, 6, 7, Table 4). Since these inhibitors are not transported by rOCT1 (Gorboulev et al., 2005; Volk et al., 2009; Koepsell et al., 2007; Nagel et al., 1997; Gorboulev et al., 1999) and passive diffusion during 1 or 5 s-incubation can be neglected, the inhibition must be due to binding of the inhibitors to the outward-open cleft of rOCT1. MPP^+ uptake mediated by wildtype rOCT1 was reduced >90% by 50 µM $TBuA^+$ (Fig. 5), >95% by 10 µM $TPeA^+$ (Fig. 6) and >95% by 200 µM corticosterone (Fig. 7). With one exception (inhibition of the mutant W218L by $TPeA^+$, Fig. 6B) the obtained inhibition curves suggest that the mutations do not diminish maximal inhibition. However, several mutations alter the affinities of the inhibitors for rOCT1 as indicated by altered IC_{50} values (Table 4). The IC_{50} values of $TBuA^+$, $TPeA^+$ and corticosterone were decreased when Asp475 was replaced by glutamate and altered after replacement of Trp218 by phenylalanine, tyrosine and/or leucine. Different effects of the mutations were observed for different inhibitors. For example, in mutant W218F the IC_{50} value for $TBuA^+$ was increased 5.3fold, the IC_{50} value for $TPeA^+$ was decreased 9fold, and the IC_{50} value for corticosterone was increased 2.7fold. Notably, largely different IC_{50} values were obtained when Trp218 was replaced by tyrosine versus phenylalanine, although the replaced amino acids only differ by one hydroxyl group. In mutant W218Y the IC_{50} for $TBuA^+$ was 10.6 times lower than in W218F while the IC_{50} values for $TPeA^+$ and corticosterone were increased 6.7 and 3.3fold, respectively. Upon exchange of Phe160 by alanine the IC_{50} values for $TBuA^+$ and corticosterone were decreased 2.3- and 2.9fold, respectively, whereas the IC_{50} value for $TPeA^+$ was not changed. The conservative exchange

of Phe160 by tyrosine only altered the IC_{50} value for $TBuA^+$, a 10fold increased concentration was required for half-maximal inhibition. In the mutant T226A the IC_{50} values for $TBuA^+$ and corticosterone were increased 6.5- and 3fold, respectively, whereas in the variant L447Y the IC_{50} values for $TPeA^+$ and corticosterone were increased 1.8- and 3fold, respectively.

For inhibition of wildtype rOCT1 and most rOCT1 mutants by $TBuA^+$, $TPeA^+$ or corticosterone, Hill coefficients around one were observed (Figs. 5-7). However, for inhibition of MPP^+ uptake by $TBuA^+$, negative cooperativity was induced after replacement of Phe160 by tyrosine, after replacement of Trp218 by phenylalanine, and after replacement of Tyr222 by phenylalanine (Fig. 5). For inhibition of MPP^+ uptake by $TPeA^+$, negative cooperativity was induced when Trp218 was replaced by phenylalanine (Fig. 6) whereas for inhibition of MPP^+ uptake by corticosterone negative cooperativity was observed in mutants F160Y, W218F and L447F (Fig. 7).

The data suggest that Asp475 and Trp218 are directly involved in binding of $TBuA^+$, $TPeA^+$ and corticosterone to the outward-open cleft, that Leu447 participates in binding of TPeA and corticosterone to the outward-open cleft, and that Phe160 is directly involved in binding of $TBuA^+$ from the extracellular side. The observation of cooperativity for inhibition of MPP^+ uptake by $TBuA^+$, $TPeA^+$ and corticosterone in some mutants suggests that rOCT1 contains more than one extracellular binding sites for each of these inhibitors. Because Thr226 has been found accessible at the inward-open but not at the outward-open cleft of our 3D structural models of rOCT1, the exchange of Thr226 by alanine in this position probably exhibits an allosteric effect on the extracellular binding site(s) of $TBuA^+$ and corticosterone.

Reevaluation of Previous Model-predicted Locations of the Phe160, Trp218, Arg440 and Asp475 within the Outward-open Cleft of rOCT1 Using a New Model of Human OCT1. The mechanisms proposed to explain the observed effects of the analysed mutations depend largely on the assigned locations of the respective residues in the outward-open cleft and hence depend on the quality of the outward-facing 3D homology rOCT1 model (Gorbunov et al., 2008; Volk et al., 2009). Our outward-facing 3D model was built manually on the basis of a 3D homology rOCT1 model in the inward-facing conformation that was modeled from the crystal structure of lactose permease (Abramson et al., 2003; Popp et al., 2005). To obtain the outward-open conformation we assumed (and

used) a rigid-body movement of the first (N-terminal) six helices with respect to the last (C-terminal) six helices, which transformed the inward-open into an outward-open conformation. Minor manual rebuilding allowing for some intrahelical motions and drifting of individual domains was necessary to remove van der Waals clashes. A very similar helix rearrangement has been proposed, modeled and also experimentally verified for lactose permease (Ermolova et al., 2006; Holyoake and Sansom, 2007; Kaback et al., 2007). Recently an outward-facing partially closed structure of hOCT1 was modeled using crystal structures of various transporters from the MFS superfamily as templates (Dakal et al., 2017). With the exception of Leu447 (with isoleucine in the corresponding position of hOCT1) the amino acids of rOCT1 investigated in this manuscript are conserved in hOCT1 (Supplemental Fig. 5). The positions of the amino acids mutated in our study that were assigned to the outward-facing cleft, are highly similar between our rOCT1 3D model and the novel 3D model of hOCT1 in an outward-facing conformation (Supplemental Fig. 6). Both models predict that Phe160, Trp218 (Trp217), Arg440 (Arg439), Leu447 (Ile446) and Asp475 (Asp474) are located within the extracellular cleft and presumably are accessible from the extracellular side. In Fig. 8 views from the extracellular space into the outward-facing cleft of our 3D rOCT1 model are presented and the mutated amino acids, which are accessible from the extracellular space, are indicated. In the model Phe160, Trp218, Arg440, Leu447 and Asp475 are surface-accessible in the outward-open cleft. Trp218 and Asp475 are located in close proximity with Phe160 and Leu447 in nearby positions. In contrast, Arg440 is located at some distance on the opposite side of the cleft.

Discussion

We report that the experimental conditions used for studying transport and inhibition of rOCT1 can have dramatic impact on effects of mutations on affinities. The data are relevant for *in vitro* characterization of drug interactions with OCTs and OCT mutants and for molecular interpretation of mutagenesis experiments. Measuring initial uptake rates under *trans-zero* conditions in stably transfected HEK293 cells, we identified interactions of inhibitors and determined probable interactions of substrates with five amino acids in the outward-open cleft of rOCT1. Trp218 and Asp475 most likely interact with the non-transported inhibitors $TBuA^+$, $TPeA^+$ and corticosterone, and presumably

also with one or two substrates (Asp475 with TEA, and Trp218 with MPP^+ and TEA^+). Phe160 most likely interacts with $TBuA^+$ and corticosterone, and probably also with MPP^+, whereas Leu447 most likely interacts with $TPeA^+$ and probably also with TEA^+. Arg440 probably interacts with TEA^+. Fitting the Hill equation to data describing the concentration dependence of MPP^+ uptake, Hill coefficients smaller than one were determined for four mutants. This suggests the existence of two transport-relevant, low-affinity MPP^+ binding sites which exhibit negative cooperativity in the respective mutants. Recent experiments support this interpretation (T. Keller, V. Gorboulev, T. Müller, V. Doetsch, J. Groll, F. Bernhard, H. Koepsell, unpublished data). Measuring MPP^+ binding to rOCT1 and rOCT1 mutants, which were reconstituted into lipid nanodiscs (Bayburt and Sligar, 2002), and measuring MPP^+ uptake into proteoliposomes containing rOCT1 and rOCT1 mutants, we observed that rOCT1 contains two low-affinity, transport-relevant MPP^+ binding sites per rOCT1 monomer which have similar dissociation constants and are located in the modeled outward-facing cleft of rOCT1.

Our interpretations concerning the interactions of the inhibitors or substrates with amino acids in the outward-open cleft are based on two or three presumptions, respectively. Firstly, it is presumed that Phe160, Trp218, Leu447, Arg440 and Asp475 are located at the inner surface of the outward-facing cleft of rOCT1 as predicted by modeling (see Fig. 8). The second presumption is that the changes in affinities observed in the mutants reflect direct effects on binding of the substrates and/or inhibitors to the respective amino acids. Our interpretation concerning the interaction of the substrates is additionally based on the presumption that the determined apparent K_m values measuring initial uptake rates reflect the binding affinities of these compounds to the extracellular-facing cleft.

Due to limited sequence homology of rOCT1 and hOCT1 to their structure templates and the fact that the conformational variability of the transporters is not known, the predictive potential of the models is inherently limited. However, considering that the models of rOCT1 and hOCT1 were derived from rather different modeling techniques and are based on quite different structure templates, the finding of highly similar positions for the five amino acid residues in the outward-facing clefts might serve as indication that these models come close to the real OCT1 structure and our first presumption is justified (see Supplemental Fig. 6).

Molecular Pharmacology Fast Forward. Published on January 16, 2018 as DOI: 10.1124/mol.117.110767
This article has not been copyedited and formatted. The final version may differ from this version.

Although a potential involvement of allosteric effects on binding of inhibitors is indicated by the observation of affinity changes of non-transported inhibitors upon mutation of Thr226, which is not accessible from extracellular (Table 4, Supplemental Fig. 6), it is more likely that the non-transported inhibitors directly interact with Phe160, Trp218, Arg440, Leu447 and Asp475. Thus, according to our model these amino acids are located at the surface of the outward-open cleft (Supplemental Fig. 6, Fig. 8), and mutating these amino acids affects both, the IC_{50} values for non-transported inhibitors and the apparent K_m values of substrates (Tables 3 and 4). In addition, the exchange of Phe160, Trp218 and Leu447 for different amino acids alters the affinities of structurally diverse non-transported inhibitors in different ways (Table 4).

The third presumption that the K_m values reflect the affinities of MPP^+ and TEA^+ binding to the outward-facing cleft, probably matches reality, because we measured initial uptake rates, and OCT1 operates as a cellular uptake system, which is supposed to have a higher affinity for extracellular substrate binding compared to intracellular substrate dissociation (Koepsell, 2011)

We showed that the experimental conditions used for *in vitro* uptake measurements in transfected HEK293 cells have dramatic effects on affinities of substrates and inhibitors. Not only apparent K_m values of rOCT1-mediated cation transport and IC_{50} values for inhibition of transport but also effects of mutations on apparent K_m values and IC_{50} values were different when uptake was measured in dissociated HEK293 cells using 1, 5 or 10 s-incubation compared to uptake measurements performed with confluent HEK293 cells using a 2 min-incubation time. The differences may be due to differing regulatory states of OCT1 in dissociated versus confluent cells, to different impact of unstirred layer effects and/or to the assessment of different transport modes. When dissociated HEK293 cells expressing rOCT1 or hOCT1 were incubated for 1-3 seconds with radioactively labeled MPP^+ performing vigorous shaking, initial linear uptake rates were determined that are higher compared to the uptake rates observed later on (Busch et al., 1996a; Minuesa et al., 2009). These initial uptake rates represent uniport involving extracellular substrate binding, substrate translocation, intracellular substrate dissociation, and reorientation of the empty transporter (Koepsell 2011). Performing a 2 min-incubation, the transport mode may change during incubation due to an increase of intracellular

Molecular Pharmacology Fast Forward. Published on January 16, 2018 as DOI: 10.1124/mol.117.110767
This article has not been copyedited and formatted. The final version may differ from this version.

substrate. This may lead to transporter-mediated efflux of radioactive substrate resulting in a slowed-down net uptake of radioactivity. It is noteworthy that the apparent linearity of radioactive uptake, which has been reported for cell layers using incubation times between 30-60 seconds and 2-5 min (Bednarczyk et al., 2003; Chen et al., 2017; Cheng et al., 2011), did not exclude higher uptake rates within the first seconds. Measuring uptake of 0.1 µM radioactively labeled MPP^+ in monolayeres of HEK293 cells stably transfected with rOCT1 or hOCT1 between 30 s-and 10 min-incubation, we observed a relatively high cell-associated MPP^+ concentration at 30 s that is most probably due to a rapid initial uptake rate (Busch et al., 1996a; Minuesa et al., 2009) and a much more slow linear uptake between 30 s and 2 min (Supplemental Fig. 7). Because mutations may change cation import and cation export differently and net uptake of radioactive substrate observed after 2 min-incubation probably reflects the difference between uptake and efflux of the radioactive substrate, it is difficult to explain functional effects of mutations observed after 2 min-incubation on the molecular level.

Recently we observed that uptake of MPP^+ in HEK293 cells stably transfected with hOCT1 was inhibited with different affinities by pentamidine, when MPP^+ was applied at different concentrations far below the apparent K_m value for MPP^+ (Minuesa et al., 2017). This indicates that the affinity of inhibitors is not only influenced by the molecular structure of the transported drug as described earlier (Thevenod et al., 2013; Belzer et al., 2013), but also by the concentration of the substrate. In the present study we showed also for rOCT1 that the inhibitor sensitivity is dependent on the substrate concentration. Furthermore, we demonstrated that the substrate concentration also influences effects of mutations on inhibitor sensitivity. We determined different IC_{50} values for inhibition of rOCT1-mediated MPP^+ uptake by $TBuA^+$ using different nanomolar concentrations of MPP^+ and showed that the influence of nanomolar MPP^+ concentrations on the IC_{50} value for $TBuA^+$ was altered differently in different OCT1 mutants. The most probable explanation for these properties of the transporter is that differing occupation of high-affinity substrate binding sites induces different allosteric effects on the transport-relevant cation binding sites and that mutations within the transport-relevant sites modulate this allosteric response.

The dramatic impact of experimental conditions on the measured affinities of substrates and inhibitors should be considered for further investigation of structure-function relationship by mutagenesis, and for *in vitro* analysis how polymorphisms influence drug affinities and drug-drug interactions at hOCT1 or the other organic cation transporter subtypes (Koepsell, 2015). To characterize the molecular impact of individual amino acids on binding or transport in mutagenesis studies defined transport modes should be analysed. For example, initial *trans-zero* uptake may be determined as performed in the present study using short-term incubation of dissociated cells including rigorous shaking to minimize unstirred layer effects. For *in vitro* characterization of effects of polymorphisms in hOCT1, human OCT2 or human OCT3 on drug transport or for *in vitro* characterizations of drug-drug interactions, conditions should be used, which reflect the *in vivo* exposition with organic cations. Hence *ín vivo* transport measured with relatively long incubation times or under equilibrium conditions is more relevant than initial uptake. Measuring the inhibition of OCT-mediated drug transport by a second drug, drug concentrations within the ranges of their free blood concentrations should be used and the tests should be extended to frequently occurring polymorphisms in the respective transporter (Koepsell, 2015).

Acknowledgements

The authors thank Irina Schatz and Alla Ganscher from the Institute of Anatomy and Cell Biology of the University of Würzburg (Germany) for expert technical assistance and Michael Christof from the Institute of Anatomy and Cell Biology of the University of Würzburg for generating the figures.

Authors Contributions

Research design: Koepsell.

Conducted experiments: Gorboulev, Rehman, Albert, Roth, Meyer, Tzvetkov, Mueller.

Performed data analysis: Rehman, Albert, Roth, Meyer, Tzvetkov, Mueller, Koepsell.

Wrote the manuscript: Koepsell.

References

Abramson J, Smirnova I, Kasho V, Verner G, Kaback H R and Iwata S (2003) Structure and mechanism of the lactose permease of *Escherichia Coli*. *Science* **301**:610-615.

Ahlin G, Karlsson J, Pedersen J M, Gustavsson L, Larsson R, Matsson P, Norinder U, Bergström C A S and Artursson P (2008) Structural requirements for drug inhibition of the liver specific human organic cation transport protein. *J Med Chem* **51**:5932-5942.

Ahlin G, Chen L, Lazorova L, Chen Y, Ianculescu AG, Davis RL, Giacomini KM and P Artursson P (2011) Genotype-dependent effects of inhibitors of the organic cation transporter, OCT1: predictions of metformin interactions. *Pharmacogenomics J* **11**:400-411.

Arndt P, Gorboulev V, Nagel G, Friedrich T, Gambaryan S, Volk C and Koepsell H (1998) Functional properties of the polyspecific rat organic cation transporter rOCT2. *Nova Acta Leopoldina NF 78* **306**:347-348.

Arndt P, Volk C, Gorboulev V, Budiman T, Popp C, Ulzheimer-Teuber I, Akhoundova A, Koppatz S, Bamberg E, Nagel G and Koepsell H (2001) Interaction of cations, anions, and weak base quinine with rat enal cation transporter rOCT2 compared with rOCT1. *Am J Physiol Renal Physiol* **281**:F454-F468.

Bayburt TH and Sligar S G (2002) Single-molecule height measurements on microsomal cytochrome P450 in nanometer-scale phospholipid bilayer disks. *Proc Natl Acad Sci U S A* **99**:6725-6730.

Bednarczyk D, Ekins S, Wikel J H and Wright S H (2003) Influence of molecular structure on substrate binding to the human organic cation transporter, hOCT1. *Mol Pharmacol* **63**:489-498.

Belzer M, Morales M, Jagadish B, Mash E A and Wright S H (2013) Substrate-dependent ligand inhibition of the human organic cation transporter OCT2. *J Pharmacol Exp Ther* **346**:300-310.

Budiman T, Bamberg E, Koepsell H and Nagel G (2000) Mechanism of electrogenic cation transport by the cloned organic cation transporter 2 from rat. *J Biol Chem* **275**:29413-29420.

Busch AE, Quester S, Ulzheimer J C, Gorboulev V, Akhoundova A, Waldegger S, Lang F and Koepsell H (1996a) Monoamine neurotransmitter transport mediated by the polyspecific cation transporter rOCT1. *FEBS Lett* **395**:153-156.

Busch AE, Quester S, Ulzheimer J C, Waldegger S, Gorboulev V, Arndt P, Lang F and Koepsell H (1996b) Electrogenic properties and substrate specificity of the polyspecific rat cation transporter rOCT1. *J Biol Chem* **271**:32599-32604.

Chen EC, Khuri N, Liang X, Stecula A, Chien H C, Yee S W, Huang Y, Sali A and Giacomini K M (2017) Discovery of competitive and noncompetitive ligands of the organic cation transporter 1 (OCT1; SLC22A1). *J Med Chem* **60**:2685-2696.

Chen L, Takizawa M, Chen E, Schlessinger A, Segenthelar J, Choi J H, Sali A, Kubo M, Nakamura S, Iwamoto Y, Iwasaki N and Giacomini K M (2010) Genetic polymorphisms in organic cation transporter 1 (OCT1) in chinese and japanese populations exhibit altered function. *J Pharmacol Exp Ther* **335**:42-50.

Cheng Y, Martinez-Guerrero L J, Wright S H, Kuester R K, Hooth M J and Sipes I G (2011) Characterization of the inhibitory effects of *N*-butylpyridinium chloride and structurally related ionic liquids on organic cation transporters 1/2 and human toxic extrusion transporters 1/2-k in vitro and in vivo. *Drug Metab Dispos* **39**:1755-1761.

Dakal TC, Kumar R and Ramotar D (2017) Structural modeling of human organic cation transporters. *Comput Biol Chem* **68**:153-163.

Egenberger B, Gorboulev V, Keller T, Gorbunov D, Gottlieb N, Geiger D, Mueller T D and Koepsell H (2012) A substrate binding hinge domain is critical for transport-related structural changes of organic cation transporter 1. *J Biol Chem* **287**:31561-31573.

Ermolova N, Madhvani R V and Kaback H R (2006) Site-directed alkylation of cysteine replacements in the lactose permease of Escherichia Coli: Helices I, III, VI, and XI. *Biochemistry* **45**:4182-4189.

Gorboulev V, Shatskaya N, Volk C and Koepsell H (2005) Subtype-specific affinity for corticosterone of rat organic cation transporters rOCT1 and rOCT2 depends on three amino acids within the substrate binding region. *Mol Pharmacol* **67**:1612-1619.

Gorboulev V, Volk C, Arndt P, Akhoundova A and Koepsell H (1999) Selectivity of the polyspecific cation transporter rOCT1 is changed by mutation of aspartate 475 to glutamate. *Mol Pharmacol* **56**:1254-1261.

Gorbunov D, Gorboulev V, Shatskaya N, Mueller T, Bamberg E, Friedrich T and Koepsell H (2008) High-affinity cation binding to organic cation transporter 1 induces movement of helix 11 and blocks transport after mutations in a modeled interaction domain between two helices. *Mol Pharmacol* **73**:50-61.

Gründemann D, Gorboulev V, Gambaryan S, Veyhl M and Koepsell H (1994) Drug excretion mediated by a new prototype of polyspecific transporter. *Nature* **372**:549-552.

Gründemann D and Koepsell H (1994) Ethidium bromide staining during denaturation with glyoxal for sensitive detection of RNA in agarose gel electrophoresis. *Anal Biochem* **216**:459-461.

Ho SN, Hunt H D, Horton R M, Pullen J K and Pease L R (1989) Site-directed mutagenesis by overlap extension using the polymerase chain reaction. *Gene* **77**:51-59.

Holyoake J and Sansom M S P (2007) Conformational change in an MFS protein: MD simulations of LacY. *Structure* **15**:873-884.

Kaback HR, Dunten R, Frillingos S, Venkatesan P, Kwaw I, Zhang W and Ermolova N (2007) Site-directed alkylation and the alternating access model for LacY. *Proc Natl Acad Sci U S A* **104**:491-494.

Karbach U, Kricke J, Meyer-Wentrup F, Gorboulev V, Volk C, Loffing-Cueni D, Kaissling B, Bachmann S and Koepsell H (2000) Localization of organic cation transporters OCT1 and OCT2 in rat kidney. *Am J Physiol Renal Physiol* **279**:F679-F687.

Koepsell H (2011) Substrate recognition and translocation by polyspecific organic cation transporters. *Biol Chem* **392**:95-101.

Koepsell H (2013) The SLC22 family with transporters of organic cations, anions and zwitterions. *Mol Aspects Med* **34**:413-435.

Koepsell H (2015) Role of organic cation transporters in drug-drug interaction. *Expert Opin Drug Metab Toxicol* **11**:1619-1633.

Koepsell H, Lips K and Volk C (2007) Polyspecific organic cation transporters: Structure, function, physiological roles, and biopharmaceutical implications. *Pharm Res* **24**:1227-1251.

Lin L, Yee S W, Kim R B and Giacomini K M (2015) SLC Transporters as therapeutic targets: Emerging opportunities. *Nat Rev Drug Discov* **14**:543-560.

Matthaei J, Kuron D, Faltraco F, Knoch T, dos Santos Pereira J N, Abu A M, Prukop T, Brockmöller J and Tzvetkov M V (2016) OCT1 mediates hepatic uptake of sumatriptan and loss-of-function OCT1 polymorphisms affect sumatriptan pharmacokinetics. *Clin Pharmacol Ther* **99**:633-641.

Minuesa G, Albert C, Pastor-Anglada M, Martinez-Picado J and Koepsell H (2017) Response to "Tenofovir disoproxil fumarate is not an inhibitor of human organic cation transporter 1". *J Pharmacol Exp Ther* **360**:343-345.

Minuesa G, Volk C, Molina-Arcas M, Gorboulev V, Erkizia I, Arndt P, Clotet B, Pastor-Anglada M, Koepsell H and Martinez-Picado J (2009) Transport of lamivudine [(-)-b-L-2´,3´-dideoxy-3´-thiacytidine] and high-affinity interaction of nucleoside reverse transcriptase inhibitors with human organic cation transporters 1, 2, and 3. *J Pharmacol Exp Ther* **329**:252-261.

Nagel G, Volk C, Friedrich T, Ulzheimer J C, Bamberg E and Koepsell H (1997) A reevaluation of substrate specificity of the rat cation transporter rOCT1. *J Biol Chem* **272**:31953-31956.

Nies AT, Koepsell H, Damme K and Schwab M (2010) Organic cation transporters (OCTs,MATEs), in vitro and in vivo evidence for the importance in drug therapy. *Handb Exp Pharmacol* **201**:105-167.

Pao SS, Paulsen I T and Saier M H, Jr. (1998) Major facilitator superfamily. *Microbiol Mol Biol Rev* **62**:1-34.

Popp C, Gorboulev V, Müller T D, Gorbunov D, Shatskaya N and Koepsell H (2005) Amino acids critical for substrate affinity of rat organic cation transporter 1 line the substrate binding region in a model derived from the tertiary structure of lactose permease. *Mol Pharmacol* **67**:1600-1611.

Thevenod F, Ciarimboli G, Leistner M, Wolff N A, Lee W K, Schatz I, Keller T, Al-Monajjed R, Gorboulev V and Koepsell H (2013) Substrate- and cell contact-dependent inhibitor affinity of human organic cation transporter 2: Studies with two classical organic cation substrates and the novel substrate Cd^{2+}. *Mol Pharm* **10**:3045-3056.

Tzvetkov MV, Saadatmand A R, Bokelmann K, Meineke I, Kaiser R and Brockmöller J (2012) Effects of OCT1 Polymorphisms on the cellular uptake, plasma concentrations and efficacy of the 5-HT(3) antagonists tropisetron and ondansetron. *Pharmacogenomics J* **12**:22-29.

Volk C, Gorboulev V, Budiman T, Nagel G and Koepsell H (2003) Different affinities of inhibitors to the outwardly and inwardly directed substrate binding site of organic cation transporter 2. *Mol Pharmacol* **64**:1037-1047.

Volk C, Gorboulev V, Kotzsch A, Müller T D and Koepsell H (2009) Five amino acids in the innermost cavity of the substrate binding cleft of organic cation transporter 1 interact with extracellular and intracellular corticosterone. *Mol Pharmacol* **76**:275-289.

Footnotes

The work was supported by the Deutsche Forschungsgemeinschaft [SFB487/A4, KO 862/6-1].

Molecular Pharmacology Fast Forward. Published on January 16, 2018 as DOI: 10.1124/mol.117.110767
This article has not been copyedited and formatted. The final version may differ from this version.

Legends to Figures

Fig. 1. Experimental conditions influence effects of mutations in rOCT1 on affinities of substrates and inhibitors. Apparent K_m values for TEA^+ and MPP^+ uptake (A), and IC_{50} values for inhibition of MPP^+ uptake by TEA^+ (B) or by $TBuA^+$ (C) mediated by rOCT1 wildtype and two rOCT1 mutants were determined using different experimental conditions as described in Table 1. I, Initial uptake of MPP^+ or TEA^+ was measured in dissociated HEK293 cells (white bars). Incubation times of 1 s (MPP^+ uptake by rOCT1 and mutant Y222F), 5 s (MPP^+ uptake by mutant D475E) or 10 s (TEA^+ uptake) were used. II, Uptake of MPP^+ was measured in monolayers of HEK293 cells using an incubation time of 2 min, shown in grey bars. III, Uptake of MPP^+ was measured in oocytes using an incubation time of 30 min, shown in black bars. The apparent K_m values and IC_{50} values determined for the mutants presented in Table I were normalized to the respective mean values determined for rOCT1 wildtype. Mean values ± S.D. of three or more experiments (see Table 1) are indicated. *P<0.05, **P<0.01, ***P<0.001 significance of difference determined by ANOVA with post hoc Tukey test; $^{\bullet}$P<0.05, $^{\bullet\bullet}$P<0.01, $^{\bullet\bullet\bullet}$P<0.001 significance of difference determined by Student´s t-test.

Fig. 2. Inhibition of MPP^+ uptake mediated by wildtype rOCT1, rOCT1(Y222F) or rOCT1(D475E) by $TBuA^+$ measured at 3 different MPP^+ concentrations far below the apparent K_m values for MPP^+. In HEK293 cells stably transfected with the rOCT1, rOCT1(Y222F) or rOCT1(D475E) initial uptake measurements of 0.25 nM, 12.5 nM or 100 nM MPP^+ in the presence of different concentrations of $TBuA^+$ were performed. Mean values ± S.D. of 3 independent experiments are indicated. The data were normalized to MPP^+ uptake in the absence of $TBuA^+$. The curves were obtained by fitting the Hill equation to the data. Mean values ± S.D. of Hill coefficients are indicated which were determined by fitting the Hill equation to individual experiments. $^{\bullet}$P<0.05 for difference to the Hill coefficient obtained for $TBuA^+$ inhibition measured with 100 nM MPP^+ determined by Student´s t-test.

Fig. 3. Substrate dependence of initial rates of MPP^+ uptake mediated by wildtype rOCT1 and rOCT1 mutants expressed in HEK293 cells. In stably transfected HEK293 cells initial uptake rates of 12.5 nM MPP^+ traced with [^{3}H]MPP^+ were measured without and with addition of nonradioactive MPP^+. The total concentrations of MPP^+ are indicated on the abscissa. Mean values ± S.D. of 3 or 4 independent experiments are shown. The data were normalized to uptake of 12.5 nM MPP^+. The replacement curves of [^{3}H]MPP^+ uptake by nonradioactive MPP^+ were obtained by fitting the Hill equation to the data. Mean values ± S.D. of Hill coefficients are indicated which were determined by fitting the Hill equation to individual experiments. $^{\bullet}P<0.05$ for difference to the Hill coefficient of wildtype rOCT1 determined by Student´s t-test. ▲Mean value of Hill coefficient is more than 2×S.D. below one.

Fig. 4. Substrate dependence of initial rates of TEA^+ uptake mediated by wildtype rOCT1 and rOCT1 mutants expressed in HEK293 cells. In stably transfected HEK293 cells initial uptake rates of 1 µM TEA^+ traced with [^{14}C]TEA^+ were measured in the presence of different concentrations of non-radioactive TEA^+. The total concentrations of TEA are indicated on the abscissa. Mean values ± S.D. of 3 or 4 independent experiments are shown. The data were normalized to uptake of 1 µM TEA^+. The replacement curves of [^{14}C]TEA^+ uptake by nonradioactive TEA^+ curves were obtained by fitting the Hill equation to the data. Mean values ± S.D. of Hill coefficients are indicated which were determined by fitting the Hill equation to individual experiments. $^{\bullet\bullet}P<0.01$ for difference to the Hill coefficient of wildtype rOCT1 determined by Student´s t-test.

Fig. 5. Inhibition of MPP^+ uptake mediated by rOCT1 wildtype or rOCT1 mutants by extracellular $TBuA^+$. In stably-transfected HEK293 cells initial uptake rates of 0.1 µM MPP^+ traced with [^{3}H]MPP^+ were measured in the absence and presence of different concentrations of $TBuA^+$. Mean values ± S.D. of 3 or 4 independent experiments are indicated. The data were normalized to MPP^+ uptake measured in the absence of $TBuA^+$. The curves were obtained by fitting the Hill equation to the data. Mean values ± S.D. of Hill coefficients are indicated which were determined by fitting the Hill equation to individual experiments. $^{\bullet}P<0.05$, $^{\bullet\bullet}P<0.01$ for difference to the Hill coefficient of wildtype rOCT1 determined by Student´s t-test.

Molecular Pharmacology Fast Forward. Published on January 16, 2018 as DOI: 10.1124/mol.117.110767
This article has not been copyedited and formatted. The final version may differ from this version.

Fig. 6. Inhibition of MPP^+ uptake mediated by wildtype rOCT1 or rOCT1 mutants by extracellular $TPeA^+$. In stably-transfected HEK293 cells initial uptake rates of 0.1 µM MPP^+ traced with [^{3}H]MPP^+ were measured in the absence and presence of different concentrations of $TPeA^+$. Mean values ± S.D. of 3 or 4 independent experiments are indicated. The measurements were performed, and the data were calculated and are presented as in Fig. 5. Student´s t-tests: $^{\bullet\bullet\bullet}P<0.001$ for difference to the Hill coefficient of wildtype rOCT1, $^{\blacktriangle\blacktriangle\blacktriangle}P<0.001$ for difference to the Hill coefficient of mutant W218Y.

Fig. 7. Inhibition of MPP^+ uptake mediated by wildtype rOCT1 or rOCT1 mutants by extracellular corticosterone. In stably-transfected HEK293 cells initial uptake rates of 0.1 µM MPP^+ traced with [^{3}H]MPP^+ were measured in the absence and presence of different concentrations of corticosterone. Mean values ± S.D. of 3 or 4 independent experiments are indicated. The measurements were performed, and the data were calculated and presented as in Fig. 5. $^{\blacktriangle}$Mean value of Hill coefficient is more than 2×S.D. below one.

Fig. 8. Views from the extracellular side on the three-dimensional structural model of the outward-facing conformation or rOCT1 with indicated positions of Phe160, Trp218, Arg440, Leu447 and Asp475. (A) Secondary structure cartoon in which the twelve transmembrane helices are shown as solid tubes and numbered accordingly. The residues are shown as sticks, with Phe160 colored in magenta, Trp218 colored in green, Arg440 shown in blue, Leu 447 indicated in yellow and Asp475 in red. (B) Surface representation of (A) using the same colour coding. (C) Surface representations of the outward-facing conformation of rOCT1 viewed from different angles in which the surface representation of Phe160 or Leu447 become visible. Trp218, Asp475 with nearby Phe160 and Leu447 form one surface patch. Arg440 in a distant location is also well accessible to the surface.

Molecular Pharmacology Fast Forward. Published on January 16, 2018 as DOI: 10.1124/mol.117.110767
This article has not been copyedited and formatted. The final version may differ from this version.

Tables

TABLE 1

Comparison of apparent K_m values and IC_{50} values of rOCT1 wildtype (WT) and two rOCT1 mutants determined under different experimental conditions. Apparent K_m values of TEA^+ and MPP^+ uptake and IC_{50} values for inhibition of uptake of 0.1 µM MPP^+ by TEA^+ or $TBuA^+$ mediated by rOCT1, rOCT1(Y222F) and rOCT1(D475E) were determined. The measurements were performed with stably transfected HEK293 cells (I, II) or with oocytes in which the transporters were expressed (III). I, Tracer uptake was measured in dissociated HEK293 cells at 37°C after incubation for 1 s (MPP^+ uptake in rOCT1 and rOCT1(Y222F)), 5 s (MPP^+ uptake in rOCT1(D475E)) or 10 s (TEA^+ uptake). In Figs. 3-5 and Supplemental Fig. 4 the compiled uptake measurements are shown. II, Tracer uptake was measured in monolayers of HEK293 cells at 37°C after incubation for 2 min. The uptake measurements are shown in Supplemental Figs. 2 and 3. III, Tracer uptake was measured in oocytes expressing rOCT1 or rOCT1 mutants after 30 min incubation at room temperature. These data are taken from our previous publications (Gorboulev et al., 1999; Gorboulev et al., 2005; Popp et al., 2005). The apparent K_m values were calculated by fitting the Michaelis-Menten equation to the data whereas IC_{50} values were calculated by fitting the Hill equation to the data. Mean values ± S.D., numbers of experiments are indicated in parenthesis.

	rOCT1	TEA^+ app..K_m [µM]	MPP^+ app. K_m [µM]	TEA^+ IC_{50} [µM]	$TBuA^+$ IC_{50} [µM]
I: HEK 1 s-uptake	**WT**	**62±7.6(4)**	**3.9 ± 0.5(4)**	**42±7.1(4)**	**0.97 0.22(4)**
II: HEK 2 min-uptake	WT	384±120(3)***	78± 9.8(3)***	639±40(3)***	8.0±1.8(3)***
III: Ooc. 30 min-uptake	WT	75±11(8)$^{\#\#\#}$	4.9 ± 1.4(4)$^{\#\#\#}$	132±21(6)***, $^{\#\#\#}$	8.2±1.8(3)***
I: HEK 1 s-uptake	**Y222F**	**59 ± 15(4)**	**5.1±1.7(3)**	**20±1.5(3)**	**0.28±0.06(3)**
II: HEK 2 min-uptake	Y222F		87± 16(3)***	526±132(3)***	0.70± 0.08(3)$^{\bullet\bullet\bullet}$
III: Ooc. 30 min-uptake	Y222F	21±1.5(4)$^{\bullet\bullet\bullet}$	9.0±0.7(3)$^{\bullet, \#\#\#}$	54±9.4(3)$^{\bullet\bullet, \#\#\#}$	6.0±1.1(3)***, $^{\#\#\#}$
I: HEK 5 s- uptake	**D475E**	**18± 5.0 (4)**	**4.8±0.9(4)**	**53±8.1(4)**	**0.49 ±0.10(3)**
II: HEK 2 min-uptake	D475E		21± 2.1(3)***	81± 17(3)*	0.50± 0.08(3)
III: Ooc. 30 min-uptake	D475E	18±1.0(3)	3.1±0.9(3)$^{\#\#\#}$	8.1±1.2(3)**, $^{\#\#\#}$	0.32±0.15(3)

*P<0.05, **P<0.01, ***P<0.001 difference to experimental condition I measured by ANOVA and post hoc Tukey test; $^{\bullet}$P<0.05, $^{\bullet\bullet}$P<0.01, $^{\bullet\bullet\bullet}$ P<0.001 difference to experimental condition I measured by Student´s t-test; $^{\#}$P<0.05, $^{\#\#}$P<0.01, $^{\#\#\#}$P<0.001 difference to experimental condition II measured by ANOVA and post hoc Tukey test.

Molecular Pharmacology Fast Forward. Published on January 16, 2018 as DOI: 10.1124/mol.117.110767
This article has not been copyedited and formatted. The final version may differ from this version.

TABLE 2

Influence on the substrate concentration used for uptake measurement on affinity of $TBuA^+$ for inhibition of MPP^+ uptake mediated by rOCT1 (WT) and two rOCT1 mutants. Initial uptake of different concentrations of MPP^+ into HEK293 cells stably transfected with rOCT1, rOCT1(Y222F) or rOCT1(D475E) was measured in the presence of different concentrations of $TBuA^+$, and the IC_{50} values for $TBuA^+$ inhibition were determined by fitting the Hill equation to data of individual experiments. Mean values ± S.D. of 3 or 4 experiments are shown. The compiled uptake measurements and the calculated Hill coefficients are shown in Fig. 2.

Transporter	IC_{50} values for inhibition of MPP^+ uptake by $TBuA^+$ using different concentrations MPP^+		
	100 nM MPP^+	12.5 nM MPP^+	0.25 nM MPP^+
rOCT1	1.14±0.04 µM	0.26±0.01 µM $^{\#\#,\ \blacksquare\blacksquare}$	0.57±0.07 µM $^{\#}$
rOCT1(Y222F)	0.30±0.03 µM ***	0.27±0.02 µM	0.36±0.14 µM
rOCT1(D475E)	0.72±0.13 µM **	0.17±0.04 µM $^{**,\ \Delta\Delta,\ \bullet\bullet\bullet}$	6.80±0.68 µM *** $^{,\#\#\#}$

ANOVA with post hoc Tukey test: **P <0.01, ***P<0.001 for difference to rOCT1 measured with the same concentration of MPP^+; $^{\#}$P<0.05, $^{\#\#\#}$P<0.001 for difference to the IC_{50} value obtained with 100 nM MPP^+; $^{\bullet\bullet\bullet}$ P<0.001, for difference to the IC_{50} value obtained with 0.25 nM MPP^+. Student´s t-test: $^{\Delta\Delta}$P<0.01 for difference to the IC_{50} value obtained with 100 nM MPP^+; $^{\blacksquare\blacksquare}$P<0.01 for difference to the IC_{50} value obtained with 0.25 nM MPP^+

Molecular Pharmacology Fast Forward. Published on January 16, 2018 as DOI: 10.1124/mol.117.110767
This article has not been copyedited and formatted. The final version may differ from this version.

TABLE 3

Apparent K_m values of MPP^+ and TEA^+ transport mediated by rOCT1 wildtype (WT) and rOCT1 mutants. Initial uptake rates of 9 different concentrations radioactively traced MPP^+ or TEA^+ were measured at 37°C in stably-transfected HEK293 cells and apparent K_m values were determined by fitting the Hill equation to data of individual experiments. Mean values ± S.D. of 3 or 4 separate experiments are shown. The compiled uptake measurements and the calculated Hill coefficients are shown in Figs. 3 and 4.

rOCT1	Transport of MPP^+ app. K_m [µM]	Transport of TEA^+ app. K_m [µM]
WT	4.7±0.8	67±9.9
F160A	10.6±0.9 ***	57±8.3
F160Y	13.3±4.6 ***	84±22
W218F	5.0±1.8	230±28 ***
W218Y	0.75±0.09 $^{\Delta\Delta\Delta, \#}$	61±7.2 $^{\bullet\bullet\bullet}$
W218L	11.9±1.8 ***, $^{\bullet\bullet\bullet}$	no uptake
Y222F	5.0±1.8	55±11
T226A	8.8±1.9$^{\Delta\Delta}$	60±7.7
R440K	4.2±1.0	32±6.0$^{\Delta\Delta}$
L447F	3.1±0.7	167±23 ***
L447Y	5.6±1.5	80±6.1 $^{\square\square\square}$
D475E	4.9±2.0	19±2.9 ***

ANOVA with post hoc Tukey test: ***P<0.001 difference to wildtype, $^{\bullet\bullet\bullet}$ P<0.001, difference to W218F, $^{\square\square\square}$P<0.001 difference to L447F; Student´s t-test: $^{\Delta\Delta}$ P<0.01, $^{\Delta\Delta\Delta}$P<0.001 difference to wildtype, $^{\#}$P<0.05 difference to W218F.

Molecular Pharmacology Fast Forward. Published on January 16, 2018 as DOI: 10.1124/mol.117.110767
This article has not been copyedited and formatted. The final version may differ from this version.

TABLE 4

Inhibition of MPP^+ uptake via rOCT1 wildtype (WT) and rOCT1 mutants by three non-transported inhibitors. Uptake measurements were performed at 37°C in stably-transfected HEK293 cells using an incubation time of 1 s with exception of mutant D475E where a 5 s-incubation was performed. Uptake of 0.1 $[^3H]MPP^+$ was measured in the presence of different concentrations of $TBuA^+$, $TPeA^+$ and corticosterone. Mean values ± S.D. of 3-5 separate experiments are shown. The compiled uptake measurements and the calculated Hill coefficients are shown in Figs. 5-7.

rOCT1	$TBuA^+$ IC_{50} [µM]	$TPeA^+$ IC_{50} [µM]	Corticosterone IC_{50} [µM]
WT	0.97±0.22	0.27±0.05	6.9 ±1.57
F160A	0.42±0.04 $^{\#}$	0.19 ± 0.04	2.36±0.59 $^{\#\#}$
F160Y	9.8±1.9 ***	0.33±0.09	8.65±0.75
W218F	5.1±0.20 ***	0.03±0.01 ***	18.8±4.3**
W218Y	0.48±0.06 $^{\#,}$ •••	0.20±0.03 ••	61.5±11.6 ***, •••
W218L	5.13±1.04***	0.41±0.05 $^{\#\#,}$ •••	4.07±1.29 ••
Y222F	0.28±0.06 $^{\#\#}$	0.18±0.02	7.07±1.69
T226A	6.4±1.6 ***	0.30±0.01	20.7±6.0 **
R440K	1.28±0.38	0.26±0.05	6.00±1.39
L447F	1.40±0.29	0.51±0.09 **	8.12±2.32
L447Y	1.04±0.14	0.49±0.07 **	20.6±4.0 **, □
D475E	0.49±0.10 $^{\#}$	0.12±0.03 *	2.26±0.31 $^{\#\#}$

ANOVA with post hoc Tukey test: **P<0.01, ***P<0.001 difference to wildtype; •• P<0.01, ••• P<0.001 difference to W218F; □P<0.05 difference to L447F; Student´s t-test: $^{\#}$P<0.05, $^{\#\#}$P<0.01, difference to wildtype.

Molecular Pharmacology Fast Forward. Published on January 16, 2018 as DOI: 10.1124/mol.117.110767
This article has not been copyedited and formatted. The final version may differ from this version.

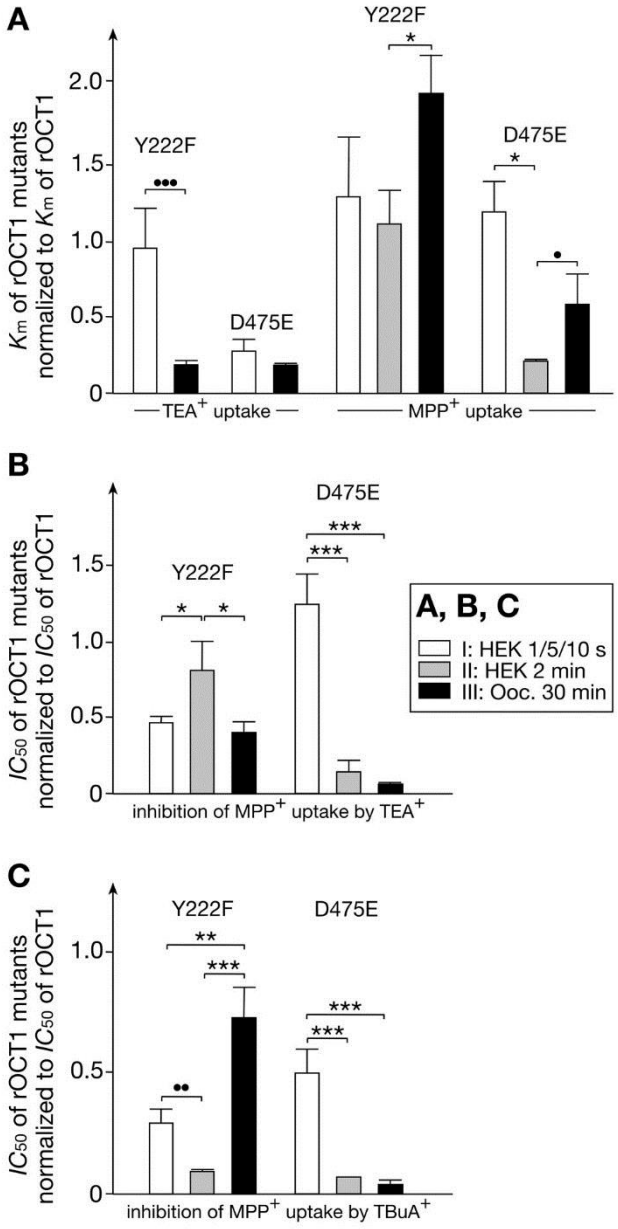

Fig. 1

Molecular Pharmacology Fast Forward. Published on January 16, 2018 as DOI: 10.1124/mol.117.110767
This article has not been copyedited and formatted. The final version may differ from this version.

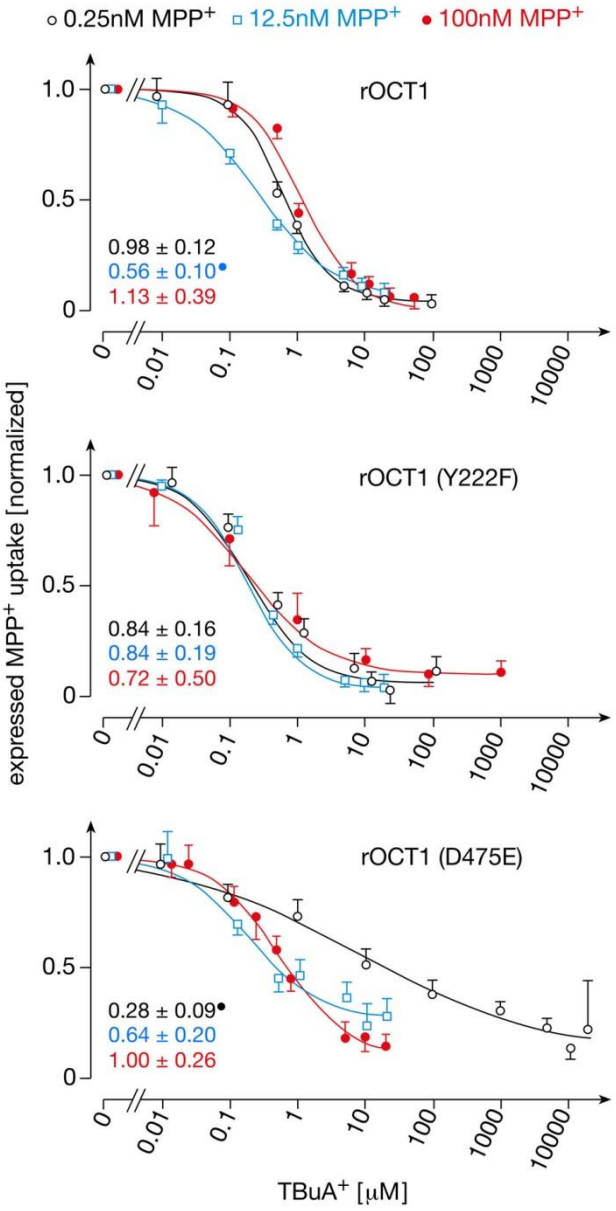

Fig. 2

Molecular Pharmacology Fast Forward. Published on January 16, 2018 as DOI: 10.1124/mol.117.110767
This article has not been copyedited and formatted. The final version may differ from this version.

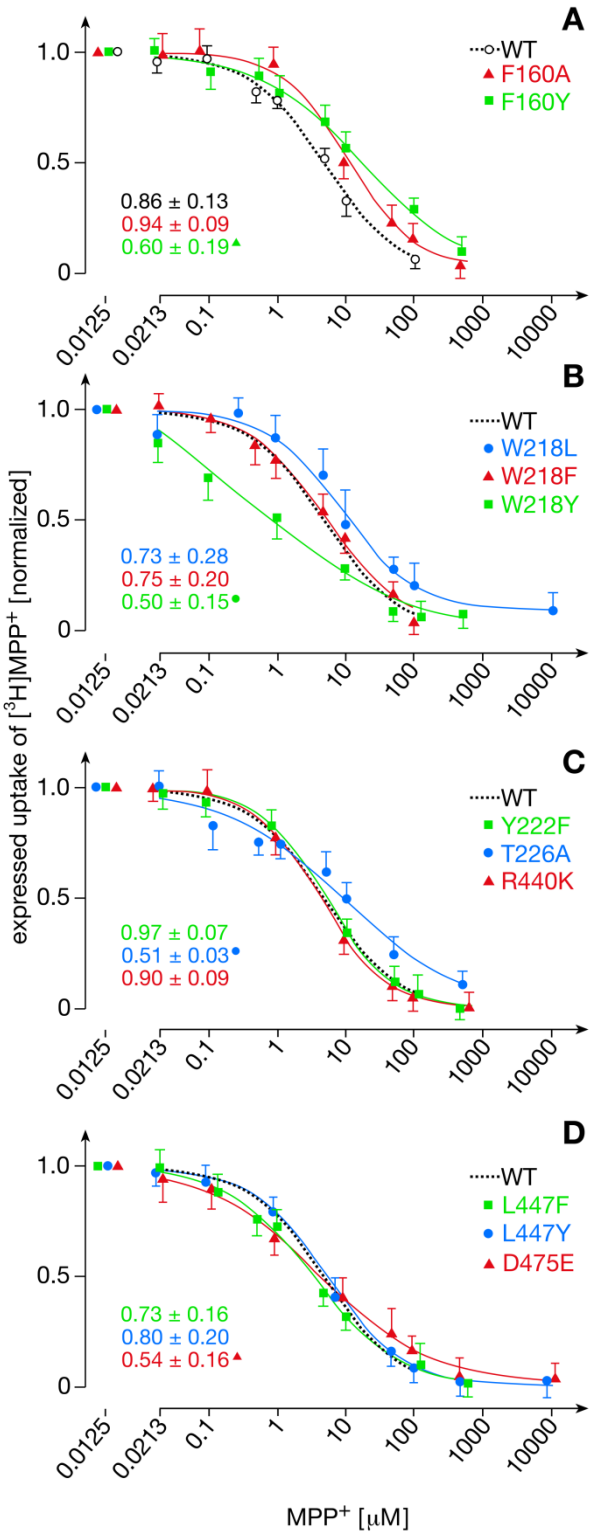

Fig. 3

Molecular Pharmacology Fast Forward. Published on January 16, 2018 as DOI: 10.1124/mol.117.110767
This article has not been copyedited and formatted. The final version may differ from this version.

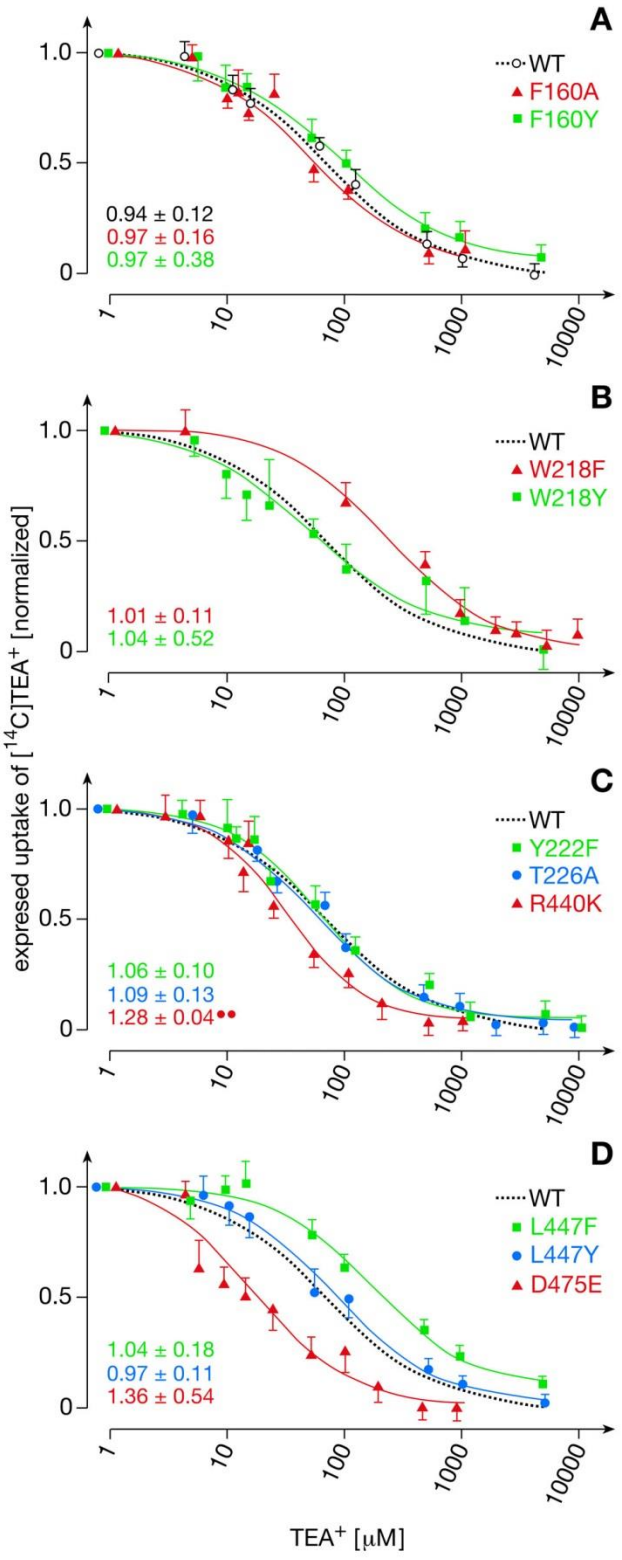

Fig. 4

Molecular Pharmacology Fast Forward. Published on January 16, 2018 as DOI: 10.1124/mol.117.110767
This article has not been copyedited and formatted. The final version may differ from this version.

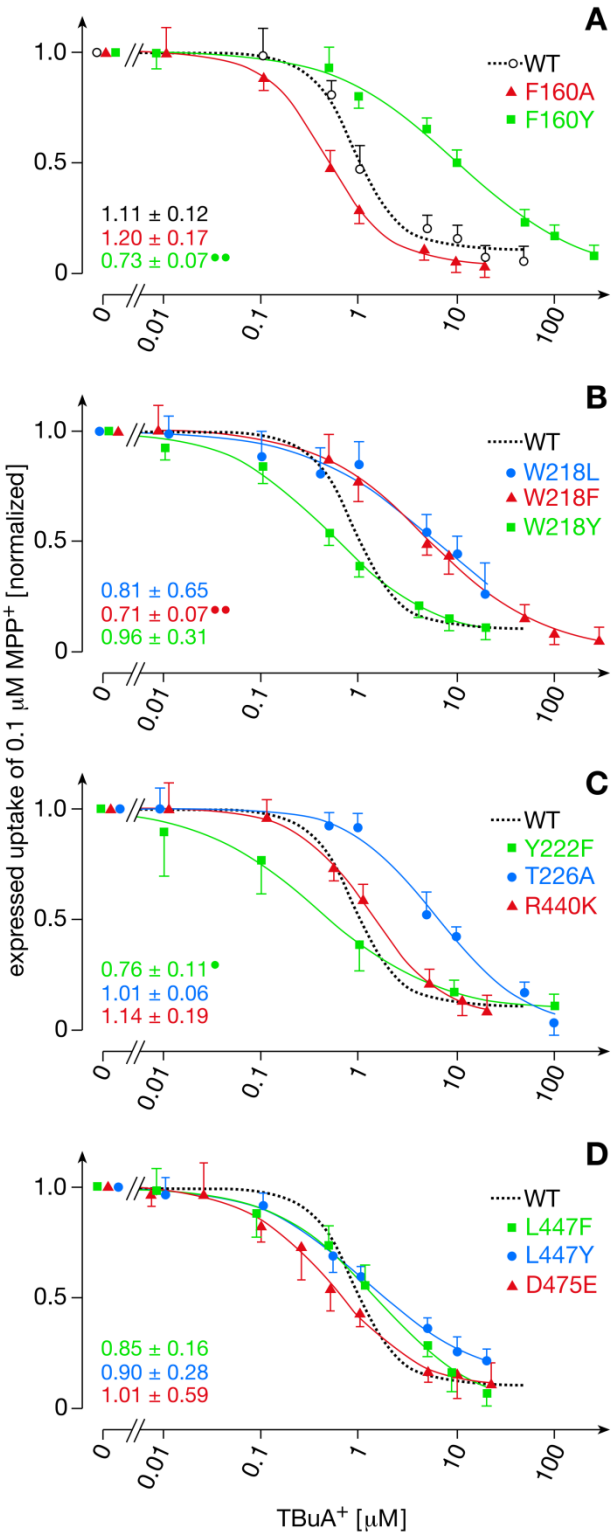

Fig. 5

Molecular Pharmacology Fast Forward. Published on January 16, 2018 as DOI: 10.1124/mol.117.110767
This article has not been copyedited and formatted. The final version may differ from this version.

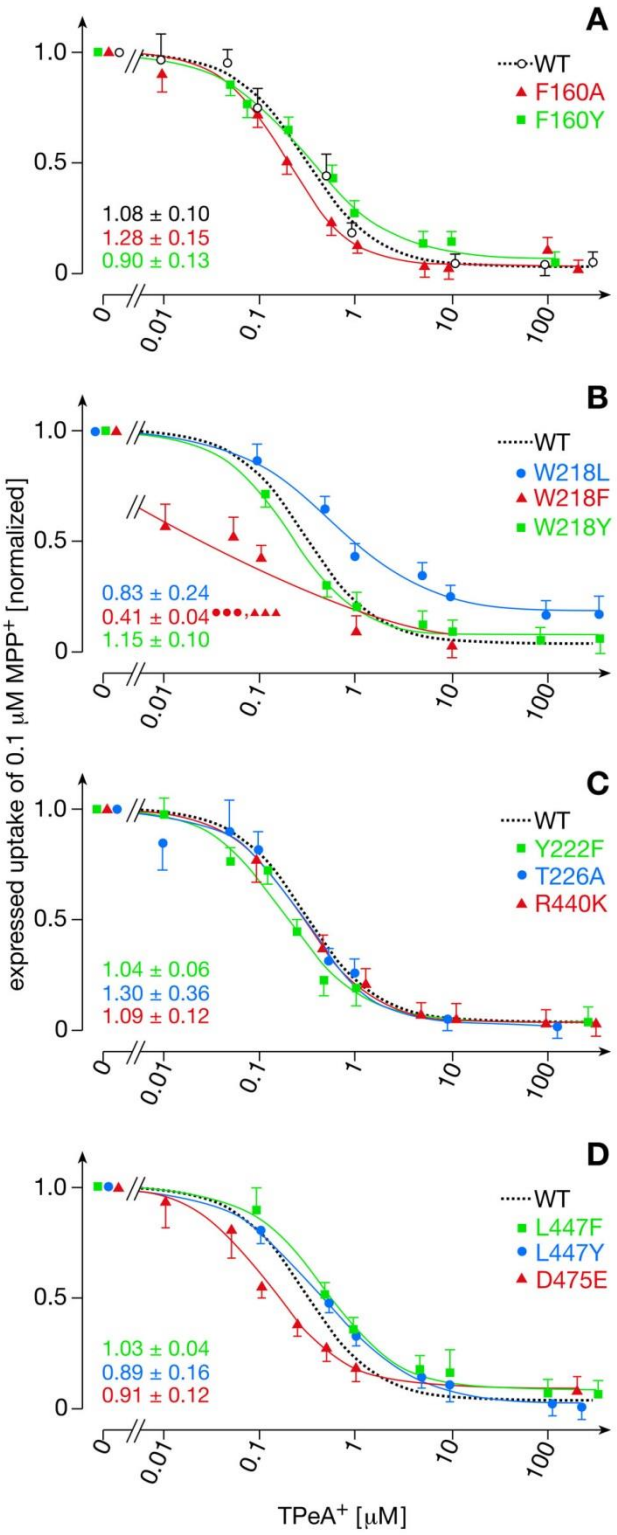

Fig. 6

Molecular Pharmacology Fast Forward. Published on January 16, 2018 as DOI: 10.1124/mol.117.110767
This article has not been copyedited and formatted. The final version may differ from this version.

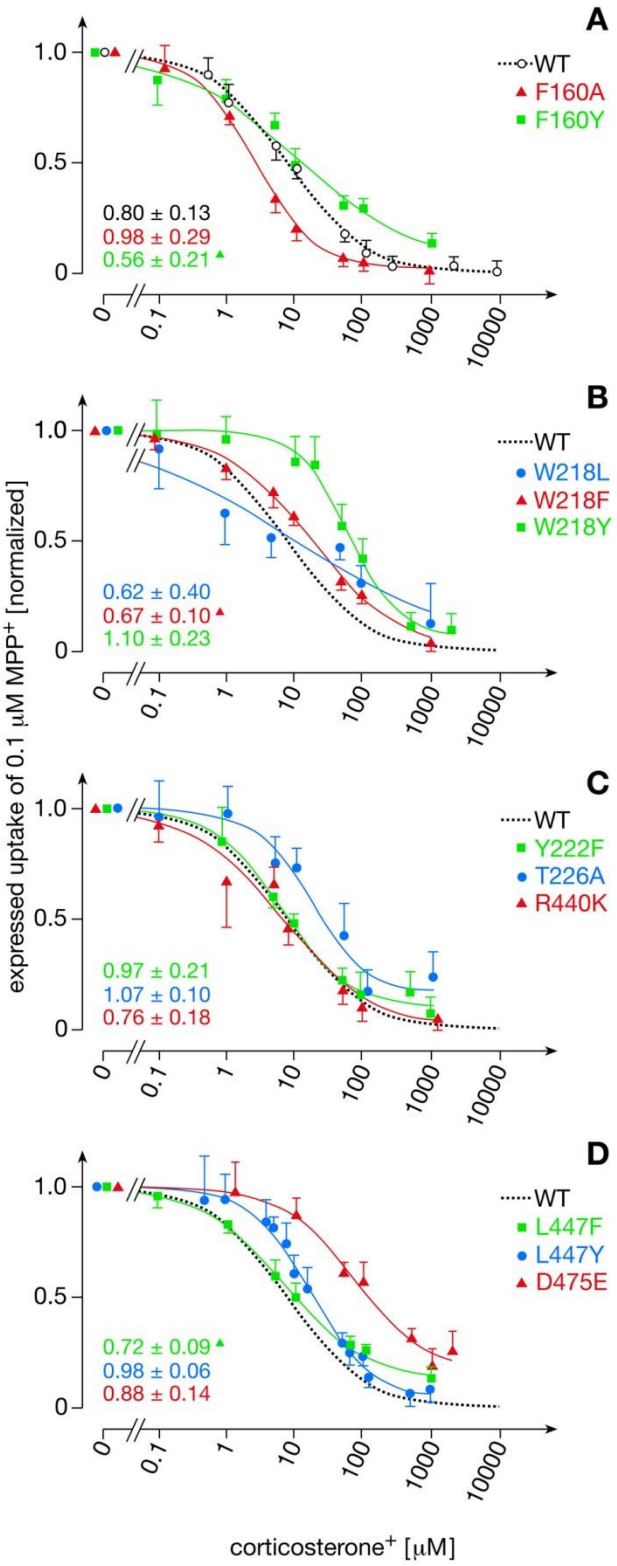

Fig. 7

Molecular Pharmacology Fast Forward. Published on January 16, 2018 as DOI: 10.1124/mol.117.110767
This article has not been copyedited and formatted. The final version may differ from this version.

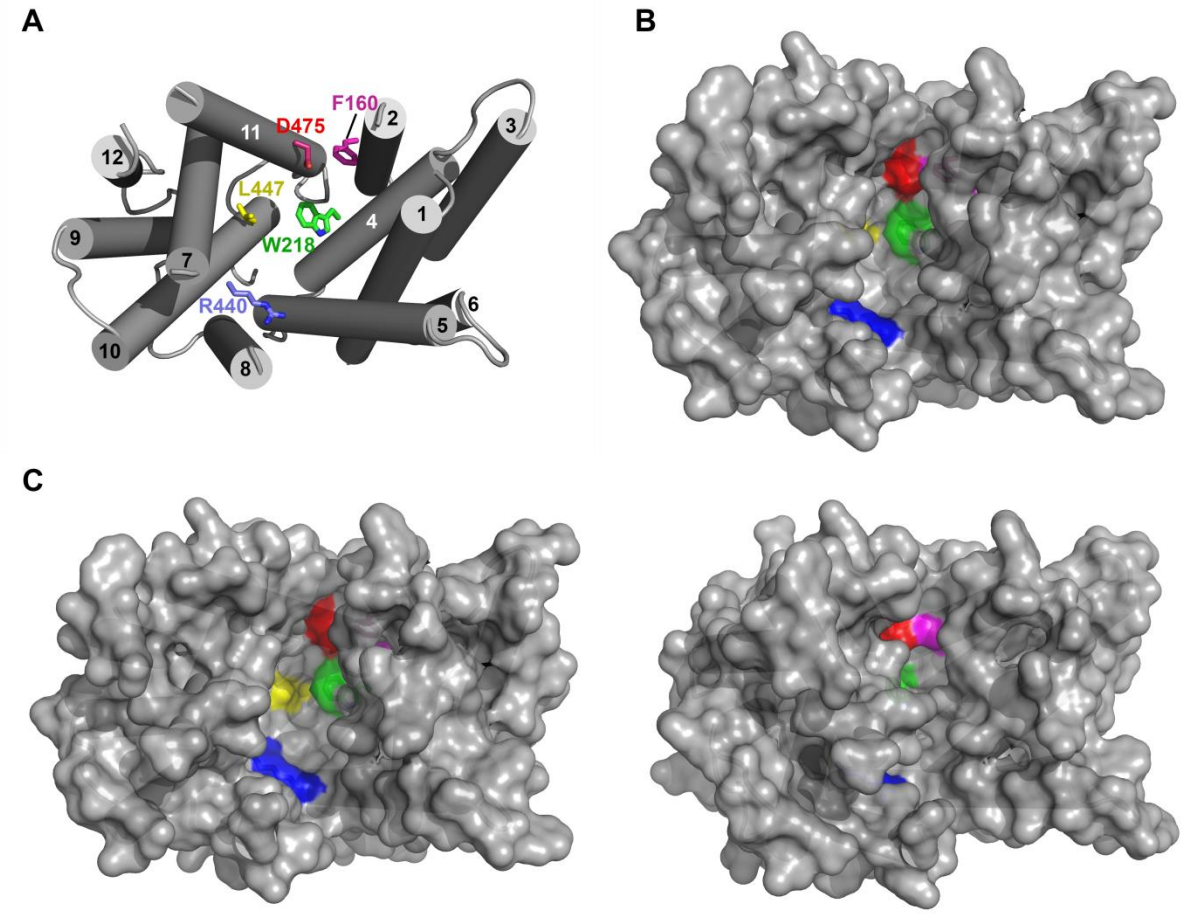

Fig. 8